

ICM11

Simulation of debonding in Al/epoxy T-peel joints using a potential-based cohesive zone model

Marco Alfano^{a,*}, Franco Furgiuele^b, Gilles Lubineau^a, Glaucio H. Paulino^c

^aCOHMAS Laboratory, Division of Physical Science and Engineering, King Abdullah University of Science and Technology (KAUST), Thuwal 23955-6900, Kingdom of Saudi Arabia

^bDepartment of Mechanical Engineering, University of Calabria, Via P. Bucci 44C, 87036 Rende (CS), Italy

^cDepartment of Civil and Environmental Engineering, University of Illinois at Urbana-Champaign, 205 N. Matthew Avenue, Urbana, IL 61801, USA

Abstract

In this work, a cohesive zone model of fracture is employed to study debonding in plastically deforming Al/epoxy T-peel joints. In order to model the adhesion between the bonded metal strips, the Park-Paulino-Roesler (PPR) potential based cohesive model (*J Mech Phys Solids*, 2009;57:891-908) is employed, and interface elements are implemented in a finite element commercial code. A study on the influence of the cohesive properties (i.e. cohesive strength, fracture energy, shape parameter and slope indicator) on the predicted peel-force *versus* displacement plots reveals that the numerical results are mostly sensitive to cohesive strength and fracture energy. In turn, these parameters are tuned until a match between experimental and simulated load displacement curves is achieved.

© 2011 Published by Elsevier Ltd. Open access under [CC BY-NC-ND license](https://creativecommons.org/licenses/by-nc-nd/4.0/).

Selection and peer-review under responsibility of ICM11

Keywords: T-peel joint, cohesive zone model, bond toughness, fracture

1. Introduction

Metal adhesive bonding is a valid alternative to the traditional joining techniques (e.g. riveting or welding). It offers the potential of reduced weight and cost, and it has found widespread acceptance in many engineering fields. The lightweight materials currently employed for the design of multi-material components, e.g. Al and Mg alloys, can greatly benefit from the advantageous properties offered by adhesive bonding. However, in order to achieve good adhesion, substrates need to be properly pre-treated so that interactions between the adherents and adhesives are promoted. From this standpoint, it has been recently demonstrated that the strength of

*Corresponding author. Tel.: +966-(0)-2-808-2137/4923

Email address: marco.alfano@kaust.edu.sa (Marco Alfano)

adhesive joints can be greatly enhanced using a pulsed laser surface treatment [1, 2]. Indeed, improved maximum load and elongation at failure were observed with respect to samples treated with traditional grit-blasting. However, the enhancement of bond toughness of the joints was not determined. As this is a key parameter for most structural models of joints and interfaces [3–8], it is of interest to determine its modification. The aim of the paper is therefore to complement those preliminary results. For this reason, a mode I cohesive model is defined which correlates the tensile traction and the displacement jump (crack faces opening) along the fracture process zone. The cohesive model is based on the Park-Paulino-Roesler (PPR) unified potential [9], and it is herein employed to simulate crack propagation in Al/epoxy T-peel joints with laser irradiated substrates. In the PPR model, four independent parameters describe the fracture behavior (delamination in our context): the cohesive strength (σ_{max}), the fracture energy (ϕ_n), the shape parameter (α) and the slope indicator (λ_n). These parameters are determined by comparing the measured peel-force *versus* displacement curves with their numerical counterparts obtained through the finite element simulations.

2. Potential based cohesive model for the analysis of debonding

2.1. Theoretical background

The cohesive model is based on the unified potential for mixed mode cohesive fracture proposed in [9]. For mode I fracture the potential, $\Psi(\Delta_n)$, can be expressed in the following form

$$\Psi(\Delta_n) = \phi_n + \Gamma_n \left(1 - \frac{\Delta_n}{\delta_n}\right)^\alpha \left(\frac{m}{\alpha} + \frac{\Delta_n}{\delta_n}\right)^m \tag{1}$$

where Δ_n is the normal opening displacement, Γ_n is the energy constant

$$\Gamma_n = -\phi_n \left(\frac{\alpha}{m}\right)^m, \tag{2}$$

m the non-dimensional exponent

$$m = \frac{\alpha(\alpha - 1)\lambda_n^2}{(1 - \alpha\lambda_n^2)}, \tag{3}$$

and δ_n is the final crack opening width

$$\delta_n = \frac{\phi_n}{\sigma_{max}} \alpha \lambda_n (1 - \lambda_n)^{\alpha-1} \left(\frac{\alpha}{m} + 1\right) \left(\frac{\alpha}{m} \lambda_n + 1\right)^{m-1}, \tag{4}$$

The intrinsic cohesive zone model for the normal cohesive stress, σ_n , is expressed in terms of normal separation, Δ_n . A schematic depiction of the intrinsic model is reported in Fig.1(a). The cohesive traction at first increases, when $\Delta_n = \delta_{nc}$ it reaches a maximum (i.e. the cohesive strength), then it softens¹ and falls to zero when the opening normal displacement reaches the final crack opening width. In the present work the traction-separation relation for normal debonding is obtained from the PPR potential (Eq. 1) as follows

$$\sigma_n = \frac{\partial \Psi}{\partial \Delta_n} = \frac{\phi_n}{\delta_n} \left(\frac{\alpha}{m}\right)^m \left(1 - \frac{\Delta_n}{\delta_n}\right)^{\alpha-1} \left(\frac{m}{\alpha} + \frac{\Delta_n}{\delta_n}\right)^{m-1} (\alpha + m) \frac{\Delta_n}{\delta_n}, \tag{5}$$

and it is plotted for various sets of parameters in Fig. 1(b); in particular, it is possible to appreciate the influence of the shape parameter on the softening behavior. Summing up, the overall cohesive parameters which need to be determined are: $\phi_n, \sigma_{max}, \lambda_n, \alpha$.

¹Note that the specific shape of the softening curve depends on the chosen value of the shape parameter (α).

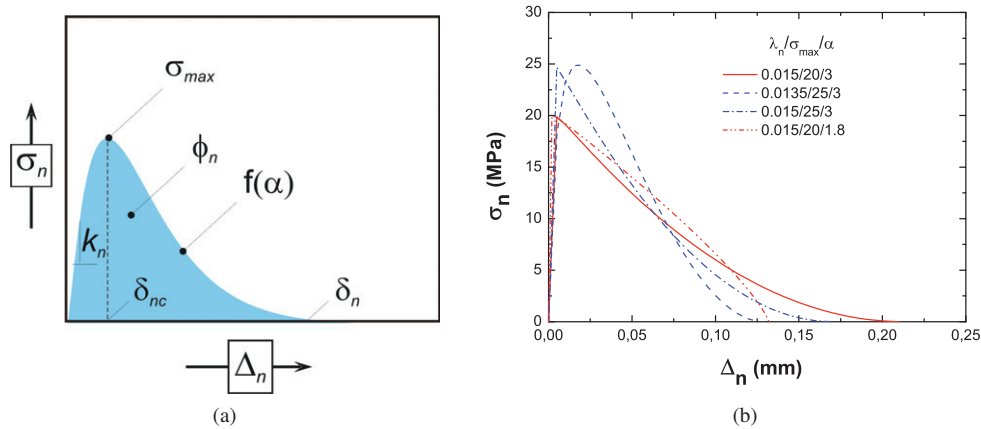


Figure 1: (a) Illustrative intrinsic traction separation relation with the associated cohesive parameters; (b) PPR based intrinsic cohesive relation of normal debonding for various combinations of fracture parameters ($\phi_n=1.5$ N/mm, σ_{max} is expressed in [MPa]).

2.2. Numerical implementation

The implementation of the CZM in the finite element framework requires cohesive elements for modeling crack initiation, evolution and final failure and continuum elements for the surrounding bulk material. The cohesive elements are herein formulated exploiting the principle of virtual work. The internal work done by the virtual strain ($\delta\epsilon$) in the domain (Ω) and the virtual crack opening displacement ($\delta\Delta$) along the crack line (Σ_c) is equal to the external work done by the virtual displacement ($\delta\mathbf{u}$) at the traction boundary (Σ), it follows

$$\int_{\Omega} \delta\epsilon^T \boldsymbol{\sigma} d\Omega + \int_{\Sigma_c} \delta\Delta^T \mathbf{T} d\Sigma_c = \int_{\Sigma} \delta\mathbf{u}^T \mathbf{P} d\Sigma, \tag{6}$$

where \mathbf{T} is the traction vector along the cohesive zone and \mathbf{P} is the external traction vector. The crack face opening is interpolated to the Gauss integration points by means of standard shape functions, i.e.

$$\left[\int_{\Omega} \mathbf{B}^T \mathbf{E} \mathbf{B} d\Omega - \int_{\Sigma_c} \mathbf{N}_c^T \frac{\partial \mathbf{T}}{\partial \Delta} \mathbf{N}_c d\Sigma_c \right] \mathbf{d} = \int_{\Sigma} \mathbf{N}^T \mathbf{P} d\Sigma \tag{7}$$

where \mathbf{N} and \mathbf{N}_c are matrices of shape functions for bulk and cohesive elements, respectively; \mathbf{B} is the derivative of \mathbf{N} ; \mathbf{d} are nodal displacements and \mathbf{E} is the material tangential stiffness matrix for the bulk elements. The stiffness matrix and load vector of the cohesive elements are assembled in a user-defined subroutine within the commercial FE code ABAQUS/Standard.

3. Analysis of debonding of T-peel Al/epoxy joints with laser treated substrates

3.1. Problem statement and modeling approach

The sample analyzed in the present work is a T-peel aluminum (AA6082T6) joints bonded with a bi-component epoxy adhesive (Loctite Hysol 9466). The Young modulus of the adhesive

provided by the manufacturer is $E_a=1.7$ GPa and the Poisson ratio is assumed to be $\nu_a=0.35$, which is a typical value measured for epoxy adhesives. The mechanical stress-strain curve of the aluminum alloy substrates was retrieved in the literature. The geometrical dimensions and boundary conditions of the joint are schematically depicted in Fig.2. The thickness of the adhesive layer was set to 0.25 mm and the mechanical tests were performed under quasi-static loading conditions. The finite element model of the sample was developed in ABAQUS (version 6.9-2) by using plane-strain four-nodes continuum elements for the bulk material. The stress-strain curve of the Al alloy was employed as input for the numerical simulations. In particular, the tensile behavior was generalized to multi-axial stress states assuming isotropic hardening and using the von Mises yield surface. Similarly to the works by [5, 6], the entire adhesive layer is replaced by a single row of cohesive elements with finite thickness (0.25 mm), which describes the macroscopic constitutive behavior of the bond-line (Fig.2). Using such an approach it is assumed that the role of the adhesive layer is to provide a traction-separation relation across the interface between the two adherends [6]. It was observed that for element sizes ≤ 0.1 mm the total dissipated fracture energy was mesh independent. Therefore, it has been set equal to 0.1 mm throughout the numerical simulations. A symmetrical 90° -peel test is assumed, therefore opening condition prevails and mixed mode effect can be neglected. As a consequence the macroscopic constitutive behavior of the adhesive layer is expressed as a function of the opening displacement Δ_n and is captured through the PPR model as described earlier. Note that this simplified kinematics describes the dominating peel deformation mode as constant through the thickness of the layer.

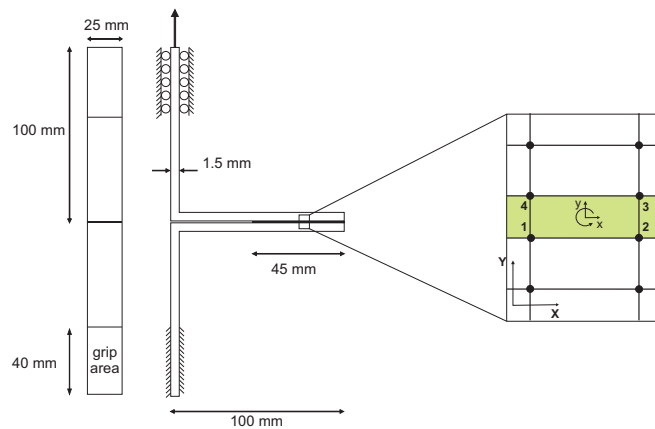


Figure 2: Geometry and boundary conditions of the T-peel sample and schematic of the mesh in the bond-line region showing finite-thickness cohesive elements.

3.2. Comparison with experiments and identification of cohesive parameters

A sensitivity analysis to cohesive fracture parameters has been performed. The influence of σ_{max} and ϕ_n on the simulated mechanical response has been firstly assessed and it is shown in Fig.3(a). It is inferred that when the σ_{max} is held constant, as ϕ_n increases the area under the curve (global dissipated energy) and the slope of the post-peak region increase. When ϕ_n is held fixed, an increase of σ_{max} causes a slight increase in the slope of the post-peak region. In both cases the increasing slope can be addressed to the leveraging effect of the adhesive toughness by plastic dissipation in the metal sheets [6]. The effect of different values of λ_n and α is shown

in Fig. 3(b). It is apparent that these parameters do not affect significantly the force *versus* displacement curve. For this reason, in the following numerical simulations, these parameters were set equal to $\alpha=3$ and $\lambda_n=0.06$, respectively.

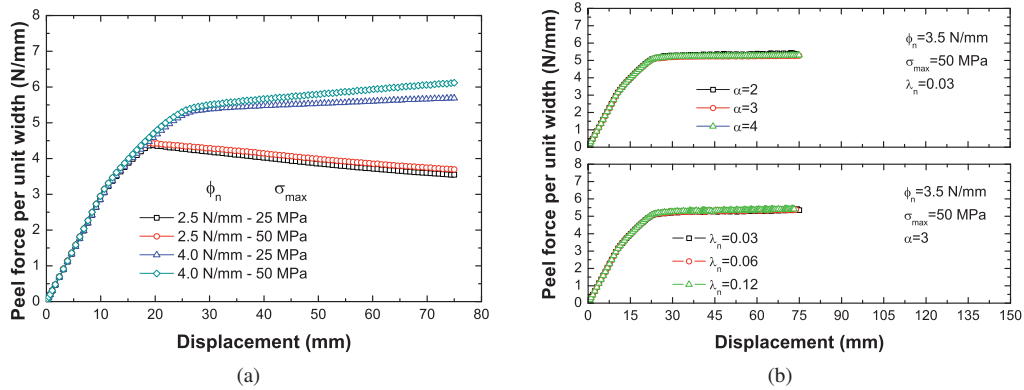


Figure 3: (a) Sensitivity of the force *versus* displacement curves to ϕ_n and σ_{max} for $\lambda_n=0.06$ and $\alpha=3$. (b) Sensitivity to λ_n and α for constant values of $\phi_n=3.5$ N/mm and $\sigma_{max}=50$ MPa.

A comparison between experimental results and numerical simulations is presented next. In particular, the experimental results pertaining to grit blasted and laser treated samples are compared in Fig.4(a). The higher scatter observed on grit blasted samples can be addressed to the poor reproducibility of this surface treatment². On the other hand there is a substantial gain in the maximum load and displacement for the laser irradiated samples. Numerical simulations which provide the best fit with the experiments are superimposed to the data reported in Fig.4(a). It is recognized that there is a range of slightly different combinations of the couple (ϕ_n, σ_{max}) providing a reasonable match between experiments and simulations. On the average the bond toughness for laser irradiated samples is four times greater than that of the grit blasted ones. This noticeable difference can be addressed to the transition from adhesive to cohesive failure³ that was observed when laser irradiation replaced traditional grit-blasting [2]. In addition, Fig.4(b) shows that the numerical simulations qualitatively reproduces the features of the deformed shape of the sample. Finally, we note that in our modeling approach the stiffness of the adhesive layer (k_n) is captured controlling the initial stiffness of the cohesive model. This last is obtained recognizing that at the initial stage of loading the normal separation is very small, and then the cohesive relation provided by Eq. 5 can be linearized in term of Δ_n

$$\sigma_n = \frac{\partial^2 \Psi}{\partial \Delta_n^2} \cdot \Delta_n = \left[\frac{\phi_n}{\delta_n^2} \left(\frac{\alpha}{m} \right)^{m+1} \left(\frac{m}{\alpha} \right)^m (m + \alpha) \right] \Delta_n = k_n \Delta_n. \quad (8)$$

It has been observed that, for the range of cohesive parameters reported in Fig.4(a), a wide variation of k_n does not affect the initial slope of the load displacement curve. Therefore, it can be concluded that the initial stiffness of the layer does not greatly affect the initial macroscopic stiffness of the joint.

²Anomalous samples responses were not considered in our analysis.

³In the context of adhesive bonded assemblies, the term *adhesive failure* is referred to interfacial fracture while *cohesive fracture* refers to fracture in the adhesive layer.

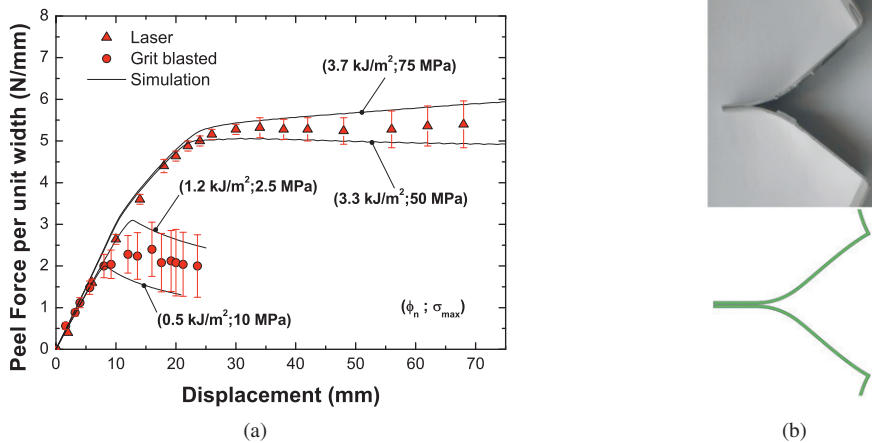


Figure 4: Comparison between numerical and experimental (a) force *versus* displacement curves and (b) deformed shape of a T-peel sample with laser irradiated substrates.

4. Conclusion

In the present work a numerical investigation on debonding in Al/epoxy T-peel joints with laser irradiated substrates has been reported in conjunction with experimental results. The numerical simulations carried out using a potential based cohesive model revealed that the bond toughness of Al/epoxy joints with laser treated substrates can be up to four times greater than that of samples with grit blasted substrates.

5. References

- [1] M. Alfano, G. Ambrogio, F. Crea, L. Filice, F. Furgiuele. Influence of laser surface modification on bonding strength of Al/Mg adhesive joints. *J Adh Sci Technol* 2011;**25**:1261-1276.
- [2] M. Alfano. An experimental study on the strenght of T-peel Al/epoxy joints with laser treated substrates. *Internal report*, University of Calabria, 2010 (available upon request).
- [3] M. Alfano, F. Furgiuele, A. Leonardi, C. Maletta, G. H. Paulino. Mode I fracture of adhesive joints using tailored cohesive zone models. *Int J Fract* 2009;**157**:193-204.
- [4] M. Alfano, F. Furgiuele, L. Pagnotta, G. H. Paulino. Analysis of fracture in aluminum joints bonded with a bi-component epoxy adhesive. *J Test and Eval* 2011;**39**(2), JTE102753.
- [5] J. L. Högberg. Mixed mode cohesive models. *Int J Fract* 2006;**141**:549-559.
- [6] Q. D. Yang, M. D. Thouless, S. M. Ward. Numerical simulations of adhesively bonded beams failing with extensive plastic deformation. *J Mech Phys Solids*, (1999);**47**:1337-1353.
- [7] A. Pirondi, F. Moroni. Clinch-bonded and rivet-bonded hybrid joints: Application of damage models for simulation of forming and failure. *J Adh Sci Technol*, (2009);**23**:1547-1574.
- [8] P. Ladeveze, G. Lubineau. Relationships between 'micro' and 'meso' mechanics of laminated composites. *Comptes Rendus Mecanique*, (2003);**331**:537-544.
- [9] K. Park, G. H. Paulino, J. R. Roesler. A unified potential-based cohesive model of mixed-mode fracture. *J Mech Phys Solids*, (2009);**57**:891-908.
- [10] M. Alfano. A potential based cohesive zone model for the simulation of failure in adhesive bonded joints. Fulbright Visiting Scholar Program, *Final Report*. University of Illinois at Urbana-Champaign, 2009 (available upon request).